Nerve Localization by Machine Learning Framework with New Feature Selection Algorithm

Oussama Hadjerci[1(✉)], Adel Hafiane[1], Pascal Makris[2], Donatello Conte[2], Pierre Vieyres[3], and Alain Delbos[4]

[1] INSA CVL, Université d'Orléans, Laboratoire PRISME EA 4229, Bourges, France
oussama.hadjerci@etu.univ-orleans.fr, adel.hafiane@insa-cvl.fr
[2] Université de Francois Rabelais, Laboratoire LI EA 6300, Tours, France
{pascal.makris,donatello.conte}@univ-tours.fr
[3] Université d'Orléans, Laboratoire PRISME EA 4229, Bourges, France
[4] Clinique Medipôle Garonne, Toulouse, France

Abstract. The application of Ultrasound-Guided Regional Anesthesia (UGRA) is growing rapidly in medical field and becoming a standard procedure in many worldwide hospitals. UGRA practice requires a high training skill. Nerve detection is among the difficult tasks that anesthetists can meet in UGRA procedure. There is a need for automatic method to localize the nerve zone in ultrasound images, in order to assist anesthetists to better perform this procedure. On the other hand, the nerve detection in this type of images is a challenging task, since the noise and other artifacts corrupt visual properties of such tissue. In this paper, we propose a nerve localization framework with a new feature selection algorithm. The proposed method is based on several statistical approaches and learning models, taking advantage of each approach to increase performance. Results show that the proposed method can correctly and efficiently identify the nerve zone and outperforms the state-of-the-art techniques. It achieves 82% of accuracy (f-score index) on a first dataset (8 patients) and 61% on a second dataset (5 patients, acquired in different period of time and not used for training).

Keywords: Feature extraction · Feature selection · Supervised learning · Nerve detection · Regional anesthesia

1 Introduction

Ultrasound-Guided Regional Anesthesia (UGRA) is becoming a major technique in pain management [17]. The forearm nerve block is one of the most important blocks used in UGRA for emergent pain control and procedural anesthesia. This block targets median, radial, and ulnar nerves. Currently, the use of UGRA in clinical practice requires a high degree of training and practical skills to identify the forearm nerve block and steer the needle to it [17]. This can limit development

V. Murino and E. Puppo (Eds.): ICIAP 2015, Part I, LNCS 9279, pp. 246–256, 2015.
DOI: 10.1007/978-3-319-23231-7_23

and generalization of the UGRA practice. The failure to locate the nerve could lead to nerve trauma or local anesthetic toxicity [20].

The aim of this work is to provide anesthetists with a tool based on ultrasound (US) image processing to facilitate the UGRA procedure. Few accurate tool detection systems have been developed in this context. In [10], a method based on the combination of a monogenic signal and a probabilistic active contour have been proposed to detect the sciatic nerve. The technique proposed in [8] is based on the combination of Median Binary Pattern (MBP) [9] and a Gabor filter to characterize and classify pixels belonging to nerve tissues.

In this paper, we focus on the median nerve, which is visible at different positions in the forearm: elbow forearm, proximal and distal forearm, and wrist forearm [18]. Figure 1 shows different types of median nerve in ultrasound image within the region of interest (ROI) outlined by anesthetists. As the median nerve exhibits a particular texture attribute, feature extraction is a required step to enable the nerve zone identification in US images. Various feature extraction methods have been recently proposed [1,3,11,14,22]. In the context of US image, extracting these features and using them to directly train a classifier is very time-consuming and may decrease the accuracy. To reduce the computational complexity and improve the accuracy, it is necessary to eliminate the redundant features and keep significant ones.

Feature selection methods can be distinguished into three categories: filter, wrapper, and hybrid methods [2]. Wrapper methods perform better than filter methods because feature selection process is optimized for a specific classifier [13]. However, wrapper methods are very time consuming for large feature space because each feature set must evaluated, that ultimately make feature selection process slow. Filter methods have low computational cost and they are faster, but with less reliability in classification as compared to wrapper methods; they are also suitable for high dimensional data sets. Hybrid methods, recently developed, use advantages of both, filter and wrapper methods. A hybrid approach using both an independent test and a performance evaluation function of features subsets, is presented in [21]. There are many algorithms of feature selection and dimensionality reduction. While these algorithms have significantly improved performance, they are still limited by the noisy data and quality of feature extraction particularly in US image.

In this paper a new hybrid approach for feature selection is proposed to identify the median nerve zone. For that purpose, 37 textural features were extracted from each ROI. Our method is based on two main approaches: ranking technique and performance predictor to evaluate the feature subsets in terms of reducing irrelevant and redundant variables. After that, Support Vector Machine (SVM) was applied with the selected features to predict the best nerve position. As we deal with three types of median nerve (elbow, proximal and distal, wrist), three SVM models have been learned to handle such variability. This yields, three nerve positions, then, a voting strategy is applied to select the best representation.

The rest of this paper is organized as follows. Section 2 describes the overall system of nerve localization, which includes different steps from pre-processing

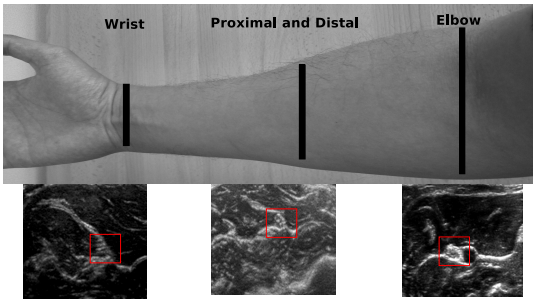

Fig. 1. Ultrasound images of the median nerve in elbow, proximal and distal, and wrist forearm.

to nerve localization. Section 3 presents experiments and results obtained from the proposed method and a comparison with other feature selection methods. Finally, conclusions are given in Section 4.

2 Nerve Detection System

In this section, we present the general framework of our system. Figure 2 shows the overall localization procedure, it consist in several image processing and machine learning techniques. First, we applied pre-processing methods to reduce the noise effect and enhance visual properties of tissues. After the pre-processing stage, feature extraction is performed to represent the texture characteristics of median nerve. In this stage 37 texture features have been obtained by several statistical measures. High number of features can inflict a heavy computational cost, and suffer from the curse of dimensionality. Furthermore, increasing the number of features may increase the risk of inclusion of irrelevant information. The aim of this stage is to select the best subset, with higher discriminative properties, from the original feature space. The optimal selected features subset, were used with SVM for learning and testing phases. Three learning SVM models were used, to handle the three median nerve positions (elbow, proximal/distal and wrist). Therefore, three candidate positions were generated. A majority vote was applied over the three candidates(ROIs), to select the best target representing the nerve.

2.1 Pre-processing

The pre-processing of US image was performed to reduce the ambiguity between the structure of nerve and epidermis. A despeckling filters was also used to reduce the degradation of the visual quality [16]. A morphological reconstruction is applied to extract the foreground region (hyperechoic tissues). Firstly, we subtract from the foreground the epidermis region, by using a skeletonization algorithm, and anatomical properties (thickness of skin (epidermis) [6]). Then

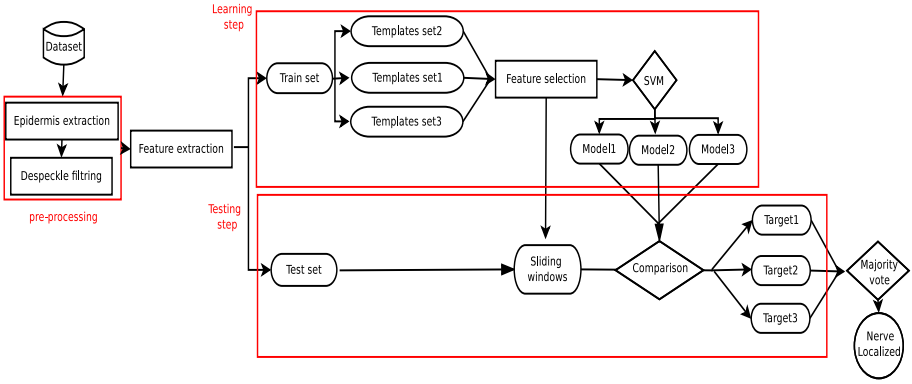

Fig. 2. Framework of median nerve localization

a despeckling filter was applied to denoise the signal of the foreground tissues. An extensive literature has recently emerged on removing the noise using different filters [12]. Most of despeckling filters are based on: linear and nonlinear filtering [16]. The linear ones showed the best result in classification and visual quality enhancement of US images [16]. In this work we adopt a linear filter that uses homogeneous mask area [19]. This filter uses two windows, the larger one is used to define the pixel neighborhood, and a moving smaller subwindow within the first main window is used to estimate the gray level homogeneity in each subwindow. The homogeneity is measured by $C = \sigma^2/\bar{M}$, where σ^2 and $\bar{M}$ are the variance and the local mean in the subwindow respectively. The center pixel value is replaced by the smallest value of C, found within the $N \times N$ search area around the center pixel. The pre-processing procedure reduce the noise and helps increasing the precision of nerve localization.

2.2 Feature Extraction

Texture information provides an important clue for nerve tissue characterization. For that purpose statistical methods were used, since they have proved to be robust in noisy data, particularly for classification of US images [16]. Hence, 37 textural features were extracted from each sliding window in US image. These features are presented in Table 1

2.3 Feature Selection

The time required for the classification increases with the number of features, and different redundant features can blur the best characterization of the nerve. Hence, this section introduces briefly some popular methods for feature selection (variable elimination), which helps to understand data, reducing computational requirements, reducing the effect of the curse of dimensionality and improving the prediction performance. Feature selection techniques can be categorized

Table 1. Feature extraction methods

Method	Extracted features
First Order Statistics (FOS)	Mean(m), median variance($\mu 2$) skewness($\mu 3$), kurtosis($\mu 4$) and speckle index(μ/m).
Gray Level Difference Statistics (GLDS) [22]	Energy, entropy, contrast, mean and homogeneity.
Neighborhood Gray Tone Difference Matrix (NGTD) [1]	Coarseness, contrast, busyness, complexity and strength
Spatial Gray level Dependence Matrices (SGLDM) [11]	Angular second moment, contrast, correlation, sum of squares, variance, inverse difference moment, sum average, sum variance, sum entropy, entropy, difference variance, difference entropy and information measures of correlation
Statistical Feature Matrix (SFM) [3]	Coarseness, contrast, periodicity and roughness
Laws Texture Energy Measures (TEM) [14]	Average gray level (L), edges (E), spots (S), waves (W) and ripples (R).

into three classes [7]: filter based, wrapper based, and hybrid methods. Filters methods can be further separated into two groups, namely (1) feature weighting algorithms, (2) subset search algorithms. Feature weighting algorithms assign weights to features individually and rank them based on their relevance with respect to the application [23], the most used feature weighting algorithms are: mutual information, Relief, information gain, Chi-square score. Subset search algorithms use a search techniques to explore different possible feature subsets and then applies statistical measures to each subset to find their merit [15]. The most popular one and widely used subset search algorithms is the correlation feature selection algorithm. Table 2 shows equations for ranking features proposed by several algorithms. Here, we discuss the notation used in the table. Details can be found in specific literature. X and Y are two random variables and $p(\cdot)$ is the probability density function, $H(X|Y) = -\sum_j P(y_j) \sum_i P(x_i|y_i) log_2(P(x_i|y_j))$ is the the entropy of X after observing Y and $H(X) = -\sum_i P(x_i) log_2(P(x_i))$ is the entropy of X. n_{ij} is the number of samples with the i^{th} feature value and $\mu_{i,j}$ is the mean, where $\mu_{i,j} = (n_{*j} n_{i*})/n$, n_{i*} is the number of samples with the i^{th} value of the particular feature, n_{*j} is the number of samples in class j and n is the number of all samples. The CFS uses a correlation based heuristic (H_s) to evaluate the worth of features, H_s is the heuristic of feature subset s containing k features, $\bar{r}_{cf}$ is the mean feature class correlation, and $\bar{r}_{ff}$ is the average feature inter-correlation.

Table 2. Filter based Feature Selection methods.

Filter based feature Selection methods	Equation
Mutual information (MI)	$I(X,Y) = -\sum_{x \in S_x} \sum_{y \in S_y} p(x,y) \log p(x/y) \ldots (2.3.1)$
ReliefF (RfF)	$\frac{1}{2} \sum_{t=1}^{p} d(f_{t,i} - f_{NM(x_t),i}) - d(f_{t,i} - f_{NH(x_t),i}) \ldots (2.3.2)$
Chi-square score (CS)	$\chi^2 = \sum_{i=1}^{r} \sum_{j=1}^{C} (n_{ij} - \mu_{ij})^2 / \mu_{ij} \ldots (2.3.3)$
Information gain (IG)	$Ig(X,Y) = H(X) - H(X/Y)) \ldots (2.3.4)$
Correlation feature selection (CFS)	$H_s = \frac{k\bar{r}_{cf}}{\sqrt{k+k(k-1)\bar{r}_{ff}}} \ldots (2.3.5)$

2.4 Proposed Feature Selection Algorithm

Ultrasound images are collected and outlined by anesthetists. Features of nerve and other tissues are extracted for every location in the image inside the sliding window, with a step of 5 pixel to reduce the computational time. These feature vectors are separated into train set (TrainFSet) and test set (TestFSet). In the selection stage, only the TrainFSet are used. The TrainFSet is itself separated into two sets, 3% as the training data, and the remaining one for validation. As shown in the Algorithm 1, first the training data (R^{Train}, Y^{Train}) and validation data (R^{Val}, Y^{Val}) are extracted randomly (*line 6*).

The significance of feature for (R^{Train}, Y^{Train}) is evaluated by mutual information, Relief, information gain and Chi-square score (*lines 7-10*). The features are ranked individually in descending order. Then, we obtain four ranked lists: the mutual information ranking list MI^{List}, ReliefF ranking list RfF^{List}, information gain ranking list IG^{List}, and Chi-square ranking list CS^{List}. Then, the intersection between the features in the ordered lists are kept to form FS^{List} (*line 11*). The features intersection are those present in the same rank in the four lists. In the next stage, the CFS algorithm (see Section 2.3) uses the previous ranking process to select the most highly correlated features (*line 12*). The final ranking list is obtained by selecting features that are present in results of both weighted and correlated method. This optimal features set is used to train the SVM for classification of the validation data (R^{Val},Y^{Val}), then the optimal features subset S is recorded, if the classification rate $fscore^t$ is higher than the $fscore^{t-1}$ obtained with the optimal features set in the previous iteration (*lines 13-15*). Then the step of the algorithm is repeated with a new random training set, the results of ($\bar{F}S^{list}, fscore^t$) are recorded if they are better than the previous round. This procedure is repeated until the stopping criteria is true (*line 16*). In this paper the stopping criteria is true when the classification rate is stable ($fscore^t - fscore^{t-1} < \epsilon$) or a maximum number of iterations is reached.

Algorithm 1. Random feature selection algorithm

Input: Data set of nerve ROIs and other tissues ROIs R
Label sets $Y = \{-1, +1\}$
Stopping criteria γ (Boolean Function)
Output: S_k

Initialization:
nbF; Number of subset
$Fscore = 0$; Classification rate
FS; Subset selected
repeat
  $[(R^{Train}, Y^{Train}), (R^{Val}, Y^{Val})] = RandomSelected(R, Y)$;
  MI^{List} Generate ranking list by Equation(2.3.1) with (R^{Train}, Y^{Train})
  RfF^{List} Generate ranking list by Equation(2.3.2) with (R^{Train}, Y^{Train})
  IG^{List} Generate ranking list by Equation(2.3.3) with (R^{Train}, Y^{Train})
  CS^{List} Generate ranking list by Equation(2.3.4) with (R^{Train}, Y^{Train})
  $FS^{List} = Intersection([MI, RfF, IG, CS]^{List})$;
  $\bar{F}S^{List} = CFS(FS^{List})$; Generate ranking list by Equation(2.3.5)
  $[Fscore] = Classification(\bar{F}S^{List}, (R^{Test}, Y^{Test}))$;
  if $(Fscore^t > Fscore^{t-1})$ **then**
    $S = FS^{list}$
until γ^t *is* true;
return S

2.5 Classification

The visual properties of nerve in US images are not necessarily consistent between different patients. Some changes in visual properties can occur. Furthermore, the position of the probe affects those properties. Several learning models are therefore required to handle such a situation. In the current work, three sets of US images were used as templates ($T1$, $T2$, $T3$) that represent different median nerves as shown in Figure 3. In the learning stage, we generated a model for each template using SVM algorithm, with a Gaussian kernel. To detect the nerve, SVM was applied in order to compare the sliding window at the position (i, j) in the input image (test) and the three templates. Then, we used the resulting SVM confidence measure with majority vote to determine the nerve position. To predict the nerve class, the distance between a sample X_p and the SVM hyperplane H_k was computed. The sample with the largest distance from the learned hyperplane is assigned with higher degree of confidence. Let be $P_{H_k} = argmax_{p=1..M} D(X_p, H_k)$, where D is the distance value assigned by the hyperplane H_k to the sample X_p, and P_{H_k} represent the largest distance. As we have three models of training, the result of the confidence measure technique yields three positions of the nerve region (P_{H_1}, P_{H_2}, P_{H_3}). Then, majority vote technique was applied to identify the most reliable region of the nerve between the three positions resulting from SVM. If the intersection of the three regions ($R_n = \cap_{k=1,2,3} Reg(P_{H_k})$) is at least 50 %, then the nerve is represented by this

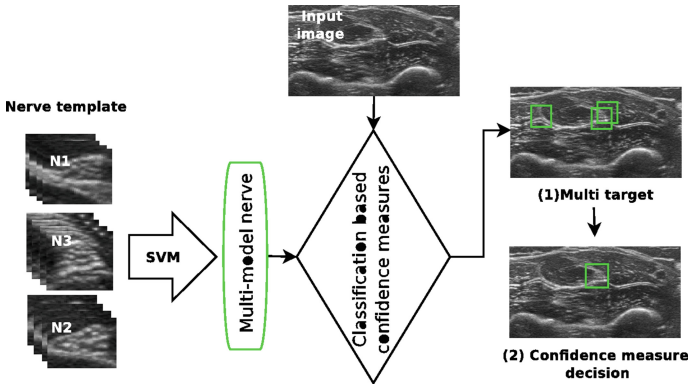

Fig. 3. Classification scheme.

intersection (R_n). Otherwise, the nerve zone is considered as the region with the highest confidence degree $P_{H_{max}} = max_{k=1,2,3}(P_{H_k})$, that is $R_n = Reg(P_{H_{max}})$.

3 Experiment Results

Sonographic video of the median nerve were obtained from 13 patients, in real conditions at the Medipôle Garonne hospital in Toulouse (France). This data are acquired in two different time periods. The first data (DS1) contains 8 patients and the second one (DS2) contain 5 patients. The probe was B-mode linear array with frequency range of 90-110 Hz for the first dataset (DS1). To evaluate the generalization of the proposed method, a second dataset (DS2) obtained from a different time period, with a frequency of 40-51 Hz, were also used for testing. To select the best frames set with different shape and texture for DS1 and DS2, 128 frames was extracted automatically by an algorithm based on the motion estimation [5]. A total of 1408 Ultrasound images of median nerve was used for the test, obtained from DS1 and DS2, and 384 ROIs obtained from DS1 was used for the training. Regional anesthesia experts validated the ground truth. The DS1 were separated into two randomly selected groups, we used one group for learning (three patients), and the remaining ones from DS1 for the tests (5 patients). DS2 were only used for testing (5 patients). For each couple of learning/testing set, the SVM algorithm has been applied to localize three ROIs per US image. For the performance measure of the proposed approach, we used the precision and recall indexes to calculate the f-score index [4]. A detected region is considered as a true positive if the intersection area of the two boxes (ground truth and detected region) divided by their union is greater than 50%. Otherwise, the detected region is considered as false positive. The false negative is incremented when it fails to give positive response, while the ground truth annotation states that there is a region of nerve. In the preprocessing

stage the despeckling filter is used; therefore, a quantitative evaluation of the proposed system without feature selection stage has been performed. We have tested different statistical features with different types of linear filters: Wiener filtering (WF), homogeneous mask area (HMA) and Mean and variance local statistics (MVLS). As illustrated in Table 3, the classification performance are represented by the average and standard deviation (i.e. $\mu \pm \sigma$) over all f-scores obtained. Compared to the state-of-the art methods, HMA despeckling filter yields the best performance to remove noise. To evaluate the testing accuracies of the proposed feature selection algorithm, we compared it with other widely used approaches: t-test, sparse multinomial logistic regression (SMLR), ReliefF, Kruskal Wallis, information gain, gain index, Fisher score, correlation feature selection (CFS), Chi-square, fast correlation based filter (FCBF), Wilcoxon test, Principal Component Analysis (PCA).

Table 3. Classification results of different linear despeckling filters.

Despeckling filter\Statistical feature	WF	HMA	MVLS
FOS	0.43 ± 0.01	0.40 ± 0.008	$\mathbf{0.52} \pm 0.04$
$GLDS$	0.25 ± 0.003	$\mathbf{0.39} \pm 0.02$	0.33 ± 0.009
$NGTDM$	0.41 ± 0.008	$\mathbf{0.47} \pm 0.005$	0.45 ± 0.006
$SGLDM$	0.59 ± 0.09	$\mathbf{0.61} \pm 0.03$	0.48 ± 0.02
SFM	0.23 ± 0.07	$\mathbf{0.34} \pm 0.005$	0.29 ± 0.01
TEM	0.53 ± 0.009	$\mathbf{0.42} \pm 0.08$	0.39 ± 0.03

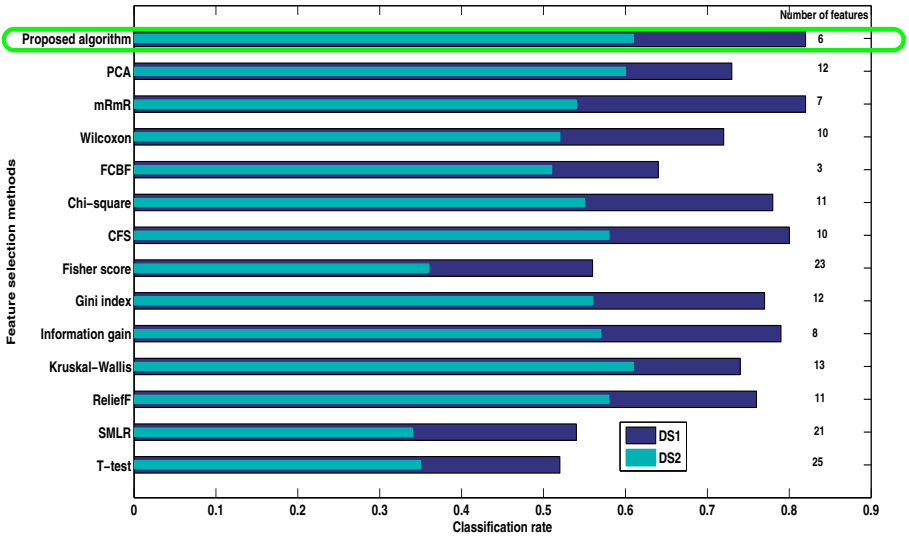

Fig. 4. Comparison of feature selection methods and the proposed algorithm

A comparison with other methods shows that the proposed method uses an equal or lower number of features to classify the median nerve with an equal or higher accuracy (see Figure 4). The highest accuracy on each dataset (DS1 and DS2) is respectively 82% and 62% and it was achieved by the proposed feature selection algorithm. The selected features in the proposed algorithm are: homogeneity, entropy, and energy derived from GLDM, strength and busyness derived from GTDM and finally the dissimilarity extracted from the SFM. The three selected statistical features can well reflect explicitly as a significant feature for classifying median nerve region and can effectively differentiate between median nerve and other tissues. Feature selection techniques show that using all information is not always good in machine learning applications. A feature selection algorithm can be chosen based on the following considerations: simplicity, stability, number of reduced features, classification accuracy, storage and computational requirements. Overall applying feature selection usually brings benefits such as providing insight into the data, better classifier model, enhance generalization and identification of irrelevant variables.

4 Conclusion

We have presented a framework based on machine learning with new feature selection algorithm to locate the nerve region for regional anesthesia application. Several texture features were extracted from ROIs, then feature selection method was used to obtain most discriminative feature set for different types of median nerve. The proposed algorithm is based on merging several feature selection approaches to improve performance. Experiments were performed in each stage of the framework, in order to evaluate the best representation of the nerve structure in ultrasound images. The proposed method can successfully identify the median nerve. These results are very helpful for the interpretation of median nerve in ultrasound images and it can increase the performance of UGRA.

Acknowledgments. This work is part of DANIEAL project supported by Region Centre-Val de Loire (France) grant 13067HPR-2013. We gratefully acknowledge Region Centre-Val de Loire for its support.l

References

1. Amadasun, M., King, R.: Textural features corresponding to textural properties. IEEE Transactions on Systems, Man and Cybernetics **19**, 1264–1274 (1989)
2. Chandrashekar, G., Sahin, F.: A survey on feature selection methods. Computer and Electrical Engineering **40**, 16–28 (2014)
3. Chung-Ming, W., Yung-Chang, C.: Statistical feature matrix for texture analysis. Graphical Models and Image **54**, 407–419 (1992)
4. Everingham, M., Van Gool, L., Williams, C.K.I., Winn, J., Zis-serman, A.: The pascal visual object classes (voc) challenge. In: IJCV, vol. II, pp. 803–806. IEEE (2010)
5. Farnebäck, G.: Two-frame motion estimation based on polynomial expansion. In: Bigun, J., Gustavsson, T. (eds.) SCIA 2003. LNCS, vol. 2749, pp. 363–370. Springer, Heidelberg (2003)

6. Frenkel, O., Mansour, K., Fischer, J.W.: Ultrasound-guided femoral nerve block for pain control in an infant with a femur fracture due to nonaccidentaltrauma. Pediatric emergency care **28**, 183–184 (2012)
7. Guyon, I.: An introduction to variable and feature selection. Journal of Machine Learning Research **3**, 1157–1182 (2003)
8. Hadjerci, O., Hafiane, A., Makris, P., Conte, D., Vieyres, P., Delbos, A.: Nerve detection in ultrasound images using median gabor binary pattern. In: Campilho, A., Kamel, M. (eds.) ICIAR 2014, Part II. LNCS, vol. 8815, pp. 132–140. Springer, Heidelberg (2014)
9. Hafiane, A., Seetharaman, G., Palaniappan, K., Zavidovique, B.: Rotationally invariant hashing of median binary patterns for texture classification. In: Campilho, A., Kamel, M.S. (eds.) ICIAR 2008. LNCS, vol. 5112, pp. 619–629. Springer, Heidelberg (2008)
10. Hafiane, A., Vieyres, P., Delbos, A.: Phase-based probabilistic active contour for nerve detection in ultrasound images for regional anesthesia. Computers in Biology and Medicine **52**, 88–95 (2014)
11. Haralick, R.M., Shanmugam, K., Dinstein, I.H.: Textural features for image classification. IEEE Transactions on Systems, Man and Cybernetics, SMC **3**(6), 610–621 (1973)
12. Joel, T., Sivakumar, R.: Despeckling of ultrasound medical images: A survey despeckling of ultrasound medical images: A survey despeckling of ultrasound medical images: A survey. Journal of image and graphic **1**(3), 161–165 (2013)
13. Kohavi, R., John, G.: Wrappers for feature selection. Artificial Intelligence **97**(1–2), 273–324 (1997)
14. Stockman, G.C., Shapiro, L.G.: Computer Vision. Prentice-Hall (2001)
15. Ladha, L., Deepa, T.: Feature selection methods and algorithms. International Journal on Computer Science and Engineering(IJCSE) **3**(5), 1787–1797 (2011)
16. Loizou, C.P., Pattichis, C.S., Christodoulou, C.I., Istepanian, R.S.H., Pantziaris, M., Nicolaides, A.: Comparative evaluation of despeckle filtering in ultrasound imaging of the carotid artery. IEEE Trans Ultrason **52**, 1653–1669 (2005)
17. Marhofer, P., Chan, V.W.S.: Ultrasound-guided regional anesthesia: current concepts and future trends. Anesth. Analg. **104**, 1265–1269 (2007)
18. McCartney, C.J.L., Xu, D., Abbas, S., Constantinescu, C., Chan, V.W.S.: Ultrasound examination of peripheral nerves in the forearm. Regional Anesthesia and Pain Medicine **32**, 434–439 (2007)
19. Nagao, M., Matsuyama, T.: Edge preserving smoothing. Comput. Graph. Image Processing **9**, 394–407 (1979)
20. Tsui, B.C., Suresh, S.: Ultrasound imaging for regional anesthesia in infants, children, and adolescents. A Review of Current Literature and Its Application in the Practice of Extremity and Trunk Blocks. Anesthesiology **112**, 473–492 (2010)
21. Veerabhadrappa, Rangarajan, L.: Bi-level dimensionality reduction methods using feature selection and feature extraction. International Journal of Computer Applications **4**, 33–38 (2010)
22. Weszka, J.C., Dyer, C.R., Rosenfield, A.: A comparative study of texture measures for terrain classification. IEEE Transactions on Systems, Man and Cybernetics **SMC–6**, 269–285 (1976)
23. Yu, L., Liu, H.: Feature selection for high-dimensional data: A fast correlation-based filter solution, pp. 856–863 (2003)